Nitric Oxide 86 (2019) 54–62

Contents lists available at ScienceDirect

Nitric Oxide

journal homepage: www.elsevier.com/locate/yniox

Cx46 hemichannel modulation by nitric oxide: Role of the fourth transmembrane helix cysteine and its possible involvement in cataract formation

Mauricio A. Retamal[a,f,g,*], Viviana P. Orellana[a], Nicolás J. Arévalo[a], Cristóbal G. Rojas[a], Rodolfo J. Arjona[a], Constanza A. Alcaíno[a,b], Wendy González[c,d], Jonathan G. Canan[c], Rodrigo Moraga-Amaro[e], Jimmy Stehberg[e], Luis Reuss[f], Guillermo A. Altenberg[f]

[a] Centro de Fisiología Celular e Integrativa, Facultad de Medicina, Clínica Alemana Universidad del Desarrollo, Santiago, Chile
[b] Enteric Neuroscience Program, Division of Gastroenterology & Hepatology, Mayo Clinic, Rochester, MN, 55905, USA
[c] Centro de Bioinformática y Simulación Molecular, Universidad de Talca, Talca, Chile
[d] Millennium Nucleus of Ion Channels-Associated Diseases (MiNICAD), Chile
[e] Laboratorio de Neurobiología, Instituto de Investigaciones Médicas, Facultad de Ciencias de la vida and Facultad de Medicina, Universidad Andrés Bello, Santiago, Chile
[f] Department of Cell Physiology and Molecular Biophysics, Center for Membrane Protein Research, Texas Tech University Health Sciences Center, Lubbock, Texas, USA
[g] Programa de Comunicación Celular en Cáncer, Instituto de Ciencias e Innovación en Medicina (ICIM), Santiago, Chile

ARTICLE INFO

Keywords:
Nitric oxide
Cataract
Hemichannels
Redox regulation
Connexins

ABSTRACT

Under normal conditions, connexin (Cx) hemichannels have a low open probability, which can increase under pathological conditions. Since hemichannels are permeable to relatively large molecules, their exacerbated activity has been linked to cell damage. Cx46 is highly expressed in the lens and its mutations have been associated to cataract formation, but it is unknown whether Cx46 has a role in non-genetic cataract formation (i.e. aging and diabetes). Nitric oxide (NO) is a key element in non-genetic cataract formation and Cx46 hemichannels have been shown to be sensitive to NO. The molecular mechanisms of the effects of NO on Cx46 are unknown, but are likely to result from Cx46 S-nitrosation (also known as S-nitrosylation). In this work, we found that lens opacity was correlated with Cx46 S-nitrosation in an animal model of cataract. Consistent with this result, a NO donor increased Cx46 S-nitrosation and hemichannel opening in HLE-B3 cells (cell line derived from human lens epithelial cells). Mutagenesis studies point to the cysteine located in the fourth transmembrane helix (TM4; human C212, rat C218) as the NO sensor. Electrophysiological studies performed in *Xenopus* oocytes revealed that rat Cx46 hemichannels are sensitive to different NO donors, and that the presence of C218 is necessary to observe the NO donors' effects. Unexpectedly, gap junctions formed by Cx46 were insensitive to NO or the reducing agent dithiothreitol. We propose that increased hemichannel opening and/or changes in their electrophysiological properties of human Cx46 due to S-nitrosation of the cysteine in TM4 could be an important factor in cataract formation.

1. Introduction

Connexins (Cxs) have four transmembrane helices (TMs), two extracellular loops, one intracellular loop, and both *N*- and C-termini regions on the cytoplasmic side (Fig. 1). Twenty genes have been associated to the expression of different Cx isoforms in mammalian cells [1]. Cxs oligomerize as hexamers to form hemichannels or connexons, which under physiological conditions have a low open probability [2]. However, under such conditions, they still allow fluxes of signaling molecules (e.g. ATP and glutamate) between the intra- and extracellular spaces [3–6]. Due to their importance in cellular communication [7,8], hemichannel opening/closing is controlled by diverse mechanisms including phosphorylation [9,10], changes of redox potential [11–13], plasma membrane depolarization [14–16], extracellular Ca^{2+}

Abbreviations: Cx, connexin; DTT, dithiothreitol; GJC, gap-junction channel; GSNO, S-nitrosoglutathione; NO, nitric oxide; SIN-1, 3-morpholinosydnonimine; SNAP, S-nitroso-*N*-acetylpenicillamine; SNP, sodium nitroprusside

* Corresponding author. Centro de Fisiología Celular e Integrativa, Facultad de Medicina, Clínica Alemana Universidad del Desarrollo, Santiago, Avenida Las Condes #12438, Chile.
E-mail address: mretamal@udd.cl (M.A. Retamal).

https://doi.org/10.1016/j.niox.2019.02.007
Received 24 October 2018; Received in revised form 8 February 2019; Accepted 20 February 2019
Available online 21 February 2019
1089-8603/

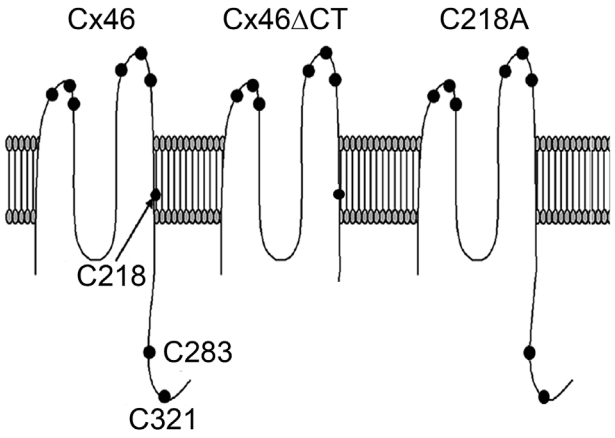

Fig. 1. Schematic representation of Cx46 and Cx46 mutants. The diagram shows the approximate location of Cx46 cysteine residues (filled circles). Cx46: wild-type rat Cx46; Cx46ΔCT: Cx46 with truncation of the C-terminal region at position 239; Cx46-C218A: mutant in which cysteine at position 218 (C218) was changed to Ala. All Cxs displayed have 6 cysteines in the extracellular loops.

concentration [17–19] and unsaturated fatty acids [20,21], among others [22,23].

The eye lens is a transparent structure critical for normal vision. Its main function is to refract light, focusing images onto the retina. Cx43, Cx46 and Cx50 are the only Cxs expressed in the lens [24]. It has been reported that cataracts (lens clouding) occur when Cx46 is absent (e.g. knockout mice) or its function is impaired by mutations [24–27]. Nitric oxide (NO) has an important role in non-genetic cataract development in humans and animal models [28–30]; it is known that increased NO levels in the aqueous humor and/or in the lens due to aging, traumatic events [31,32], diabetes [33] or hypertension [34] are closely correlated to cataract formation. The mechanism by which NO participates in the cataract formation is not completely understood, but a role of Cx46 hemichannels is possible since the NO donor S-nitrosoglutathione (GSNO) modulates Cx46 hemichannel's electrophysiological properties and permeability to large molecules, likely through S-nitrosation of at least one of its transmembrane/intracellular cysteine(s) [11].

It is unknown whether or not S-nitrosation of Cx46 occurs *in vivo* and whether this modification is associated with cataract formation. Here, we: 1) determined whether Cx46 is S-nitrosylated in response to oxidative stress in an animal model of cataract, 2) determined whether NO affects hemichannel activity in human epithelial lens cells (HLE-B3 cells), and 3) identified the functional target of S-nitrosation in Cx46. We found that lens opacity was correlated with Cx46 S-nitrosation in a rat model of selenite-induced cataracts. Consistent with this observation, NO donors increased hemichannel opening and Cx46 S-nitrosation in HLE-B3 cells. In electrophysiological studies performed in *Xenopus laevis* oocytes, NO donors caused rat Cx46 hemichannel current inactivation and gain in amplitude of the tail current, effects that were absent in hemichannels formed by a mutant where cysteine at position 218 (C218) (rat equivalent of human C212) was replaced with alanine. We propose S-nitrosation of the cysteine at the TM4 of Cx46 as an important factor for the development of cataracts because of increased hemichannel opening, and/or changes in hemichannel electrophysiological properties.

2. Methods

2.1. Ethical approval

All procedures involving animals were approved by Universidad Andres Bello Bioethical Committees. All procedures were conducted by personal trained to work with animals following local rules for animal care and in accordance to NHI guidelines.

2.2. Chemicals

Fluoromount-G was purchased from Electron Microscopy Science (Ft. Washington, PA, USA). Dithiothreitol (DTT) and sodium selenite were obtained from Sigma-Aldrich (St. Louis, MO, USA). SNAP (S-nitroso-*N*-acetylpenicillamine) and SIN-1 (3-morpholinosydnonimine) were obtained from Cayman Chemical (Ann Arbor, MI, USA), and SNP (sodium nitroprusside) and GSNO (S-nitrosoglutathione) were obtained from Merck (Darmstadt, Germany). The mouse monoclonal *anti*-S-nitrosocysteine antibody was obtained from Abcam (San Francisco, CA, USA), and the rabbit polyclonal *anti*-Cx46 antibody was purchased from Santa Cruz Biotechnology (Santa Cruz, CA, USA). For immunoprecipitation (IP) the Dynabeads Antibody Coupling kit (Life Technologies, Norway) was used.

2.3. Plasmid engineering

cDNA of rat Cx46 was obtained from Dr. Lisa Ebihara (Finch University of Health Sciences, Chicago, IL, USA) as plasmid pSP64T-Cx46 [35]. Fig. 1 shows the relative position of each cysteine in wild type Cx46 and the Cx46 cysteine mutants employed in these studies. C218A was generated by replacing the TGT codon with GCT using site-directed mutagenesis (Quick Change Multisite Site-Directed Mutagenesis kit, Stratagene, La Jolla, CA, USA). The truncation of the C-terminal domain (Cx46ΔCT, truncated after Gly 239) was described previously [36].

2.4. Selenite-induced cataract

We used male Sprague-Dawley rats, following the protocol described by Li and colleagues [37], but using rats weighting 100–150 g. Animals from the selenite-induced cataract group received a single subcutaneous injection of sodium selenite (1 mg/kg) dissolved in physiological saline solution (0.9% NaCl). Animals from the control group received a single injection of physiological saline solution. Ten days post-injection the rats were anesthetized by a subcutaneous injection of a 60.6 mg/kg ketamine, 0.6 mg/kg xilazine and 6.67 mg/kg acepromacine. Lenses were then extracted from the eye and the animals were euthanized with an overdose of anesthetics.

2.5. Confocal microscopy analysis

Immediately after extraction, the rat lenses were photographed using a stereomicroscope. The lenses were then embedded in OCT, frozen in liquid nitrogen and stored at −80 °C. Sagittal cryostat sections (10-μm thick) were prepared and then fixed by incubation with 4% paraformaldehyde for 20 min at room temperature, washed three times with PBS and stored at 4 °C. A blocking solution containing 1% IgG-free BSA, 50 mM NH_4Cl and 0.05% Triton X-100 in PBS was used for permeabilization and for blocking non-specific reactive sites. Cx46 and S-nitrosylated proteins were detected with a rabbit polyclonal *anti*-Cx46 and mouse monoclonal *anti*-S-nitrosocyteine antibodies, respectively. These primary antibodies were diluted in blocking solution and used for incubation with the samples overnight. After washing with PBS, the samples were incubated with Cy2-conjugated goat anti-rabbit (1:300) IgGF(ab') fragments and Cy3-conjugated anti-mouse IgGF(ab') fragments for 45 min at room temperature. Images were examined on a confocal laser-scanning microscope (Zeiss Spectral Confocal Microscope, LSM780, Toronto, Ontario, CA). Images of 0.2-μm optical thickness were acquired for analysis with the Zen 2011 Carl Zeiss image analysis software.

2.6. Cell culture

The human lens epithelial cell line HLE-B3 was obtained from ATCC (Rockville, MD, USA) and cultured in 60-mm-diameter dishes at 37 °C and 5% CO_2 in DMEM supplemented with 20% fetal bovine serum (FBS, GIBCO, Invitrogen) with 100 U/ml penicillin and 100 μg/ml streptomycin sulfate (Nunc, Roskilde, Denmark). For dissociation of attached cells for sub-culturing we used 0.05% trypsin-EDTA.

2.7. Dye uptake

Hemichannel activity was evaluated through the uptake of ethidium (Etd) (charge = +2, MW = 394) at a final concentration of 10 μM. HLE-B3 were grown in glass coverslips and the day of experiments a single coverslip was transferred to a 30-mm plastic dish and washed twice with recording solution of the following composition (in mM): 140 NaCl, 4 KCl, 2 $CaCl_2$, 1 $MgCl_2$, 5 glucose, and 10 HEPES, pH = 7.4. Changes in Etd fluorescence intensity were evaluated in images taken every 20 s during a 20 min period, using an inverted microscope (Eclipse Ti-U, Nikon). To induce hemichannel opening, cells were incubated in nominally divalent cation-free solution (DCFS; recording solution above, but without $CaCl_2$ and $MgCl_2$). NIS elements advanced research software (version 4.0, Nikon) was used for data acquisition and image analysis. The fluorescence intensity of 16 cells per experiment was averaged and plotted against time, and the slope of the linear rate of fluorescence increase, calculated with GraphPad Prism software version 5, was used as an indicator of the rate of Etd uptake.

2.8. Cx46 immunoprecipitation (IP)

Primary antibodies were attached to magnetic beads following the the manufacturer's instructions (Dynabeads kit, ThemoFisher #14311D). Briefly, 1 mg of magnetic beads were mixed with 10 μg of primary antibody and incubated in a roller mixer at 37 °C for 24 h. Next day, the mixture was washed three times with the kit's washing buffer. The *anti*-Cx46 attached to magnetics beads was resuspended in 100 μl of kit's buffer SB, and stored at 4 °C. Between each washing procedure, the magnetics beads were precipitated with a small magnet.

HLE-B3 cells were grown in 90 mm plastic dishes (NunClone) to 90% confluence. Then, the cells were exposed to 500 μM sodium nitroprusside (SNP) for 20 min at 37 °C, followed by harvesting and sonication in 1 ml PBS with protease inhibitors (cOmplete mini, Roche). Then, 50 μl of *anti*-Cx46 or *anti*-S-NO attached to magnetic beads was added to the cells' suspension and placed at 4 °C overnight under constant agitation, to avoid beads agglomeration. After that, the suspension was placed over a magnet and the collected magnetics beads were washed with 1 ml of PBS three times. After the final wash the magnetic beads were pelleted with the magnet, the supernatant was discharged, and 50 μl of PBS plus 100 mM glycine pH 2.0 was added to release the Cx46 bound to the antibody. The sample was mixed for 1 min, the tube was placed over the magnet, and the supernatant was collected in a tube containing 50 μl of 1 M HEPES, pH 7.0. The presence of Cx46 and S-nitrosylated proteins was examined by Western blot analysis.

2.9. Western blots

IP samples were resuspended in Laemli's sample buffer, separated on 12% SDS-PAGE, and electro-transferred to a nitrocellulose membrane using a Dry iBlot Gel Transfer System (Life Technologies). Nonspecific protein binding sites were blocked by incubation for ~60 min with TBS containing 5% nonfat milk and 0.05% Tween-20 buffer. Membranes were then incubated with primary polyclonal *anti*-Cx46 (1:1000) or *anti*-S-NO (1:100) antibodies overnight at 4 °C. Primary antibodies were diluted in TBS with 5% nonfat milk and 1% Tween-20 buffer. Next day, the membranes were washed five times with TBS containing 1% Tween-20. The membranes were then incubated with secondary antibody conjugated to horseradish peroxidase (1:2000 in TBS containing 5% nonfat milk and 0.1% Tween-20), and finally, immunoreactivity was detected on a Blot-scanner (C-Digit, Licor) for ECL using the SuperSignal kit (Pierce, Rockford, IL) according to the manufacturer's instructions.

2.10. cRNA preparation and injection into Xenopus laevis oocytes

Xenopus oocytes were obtained from female frogs (n = 6) anesthetized in a solution of tricaine methanesulfonate as described [38]. Eggs were placed in a 15-ml tube containing OR2 solution (82 mM NaCl, 3 mM KCl, 1 mM $CaCl_2$, 1 mM $MgCl_2$, and 5 mM HEPES/NaOH, pH 7.4) plus 1% collagenase for 1–2 h at room temperature, followed by three washes with OR2 solution and two washes with Bart's solution (88 mM NaCl, 1 mM KCl, 5 mM $CaCl_2$, 0.8 mM $MgCl_2$, and 10 mM HEPES/NaOH, pH 7.4). Eggs were finally placed in a 90-mm plastic dish in Bart's solution. The rat's cDNAs from Cx46, Cx46ΔCT and C218A used as templates were linearized with *Sal*I (New England Biolabs, Ipswich, MA, USA), and the cRNA was prepared using the SP6-mMessage Machine kit (Ambion, Austin, TX, USA) and stored at −20 °C. Oocytes were injected with 12.5 ng of antisense Cx38 oligonucleotide alone or in combination with 25 ng of cRNA coding for Cx46 or Cx46 mutants. After cRNA injection, the oocytes were maintained in Barth's solution supplemented with 0.1 mg/ml gentamycin and 20 units/ml of penicillin-streptomycin each for 24–48 h to allow for a good level of Cx expression.

2.11. Electrophysiological recordings

Whole-cell hemichannel currents were measured as described elsewhere [36]. Briefly, oocytes were placed in a 1-ml recording chamber and superfused with ND96 solution (96 mM NaCl, 2 mM KCl, 1.8 mM $CaCl_2$, and 5 mM HEPES/NaOH, pH 7.4) at room temperature. We used the pClamp 10/Digidata 1440A A/D Board (Molecular Devices, Foster City, CA, USA) for data acquisition and analysis. Currents were measured following 15-s rectangular voltage pulses ranging from −50 mV to +60 mV, in 10-mV steps, with a holding potential of −60 mV and 10-s intervals between pulses. Oocytes were incubated with NO donors (GSNO, SIN-1, SNAP and SNP), then washed twice with 2 ml of ND96 and placed in the recording chamber. Oocytes incubated in 10 mM DTT were washed with 2 ml of ND96 before recordings. All recordings and incubations were performed at room temperature.

Currents through gap-junctional channels (GJCs) were measured in paired oocytes. Both cells were clamped at −40 mV, and gap junctional currents were measured after changing the cell-membrane voltage of one cell to values between −140 and + 60 mV (20 mV steps, 15-s intervals between pulses), while holding constant the voltage of the other cell (used as reference). To evaluate the effects of NO donor, 500 μl of NO donor was prepared in ND96 to a final concentration of 1 mM and carefully added to the 4.5-ml recording chamber. Recordings were performed after 20 min of incubation with the NO donor.

2.12. Cx46 molecular modeling

A Cx46 homology model was built using ICM [39] based on the structure of Cx26 (PDB ID: 2ZW3) [40]. The homology model of Cx46 was validated using RAMACHANDRAN plot [41], RMSD values [42] and HOLE calculation [43]. The homology model was embedded into a pre-equilibrated 1-palmitoyl-2-oleoyl-*sn*-glycero-3-phosphocholine (POPC) bilayer in a periodic boundary condition box (124 × 123 × 129 Å) with pre-equilibrated TIP3P water molecules [44]. The system was ionized with 30 mM $CaCl_2$. The initial configuration of the system was first optimized using energy minimization followed by a molecular dynamics (MD) simulation at 310 K for 10 ns. The MD simulations were done in an isobaric-isothermal ensemble using harmonic restraints of 1 kcal/mol applied to the protein backbone

atoms. During the first 3.8 ns the harmonic restraints were decreased trough cycles from 1 to 0.5 kcal/mol. For the rest of the MD simulations the restraints of 0.5 kcal/mol to Cx46 backbone atoms were maintained. All MD simulations were performed using the NAMD program [45] and CHARMM force field.

2.13. Statistics

Results are expressed as means ± SEM, and "n" refers to the number of independent experiments. For statistical analysis, each treatment was compared to its respective control, and significance was determined using a one-way ANOVA or paired Student's t tests, as appropriate. Differences were considered significant at $P < 0.05$.

3. Results

3.1. Cx46 is S-nitrosylated in an animal model of cataract

Cx46 is mainly expressed in the lens [46] and mutations in its gene that induce changes in the properties of both hemichannels and GJCs have been correlated with cataract formation [46]. On the other hand, Cx46 hemichannel oxidation by NO leads to changes in hemichannel properties *in vitro* [36]. However, it is unknown if S-nitrosation of Cx46 occurs *in vivo* and whether it is associated with cataract formation. To address this issue, we evaluated whether Cx46 is S-nitrosylated in a selenite-induced cataract model [47,48]. Adult rats were exposed to sodium selenite for 10 days and their lens transparency was studied. Under control conditions (rats injected with saline solution) the lenses were transparent (Fig. 2A, left panel), whereas in rats injected with selenite the lenses presented extensive opaque zones (Fig. 2A, right panel). To determine Cx46 S-nitrosation we used antibodies that detect S-nitrosylated proteins and rat Cx46. Under control conditions, a green immunofluorescence corresponding to Cx46 was detected, with no signal from S-nitrosylated proteins (Fig. 2B, Control). No evident changes in intensity and distribution of the Cx46 signal were observed after 10 days of exposure to selenite, but a clear signal indicating the presence of S-nitrosylated proteins was detected (Fig. 2B, Selenite). Co-localization of Cx46 and S-nitrosation was observed (Fig. 2B, Selenite), suggesting that in this cataract model Cx46 is S-nitrosylated.

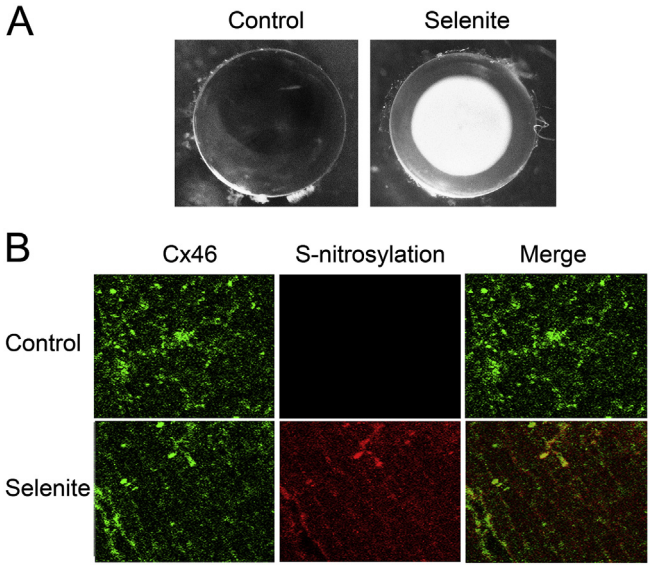

Fig. 2. Cx46 S-nitrosation may be associated with cataracts in an animal model. Male Sprague-Dawley rats received a single subcutaneous injection of sodium selenite (1 mg/kg) or vehicle (saline solution 0.9% NaCl). Ten days post-injection lenses were extracted and their transparency was analyzed. (A) Representative images of lenses from rats under control condition (left) or injected with sodium selenite (right) (n = 6 animals per condition) (B) Immunofluorescence analysis of Cx46 (green) and S-nitrosylated proteins (red) in the lenses showed in A. The merged images are also shown.

3.2. NO increases hemichannel opening and Cx46 S-nitrosation in HLE-B3 cells

Since Cx46 hemichannel properties are affected by NO [12,36] and the protein is S-nitrosylated in a rat model of cataracts (see above), we determined whether NO donors alter permeation through hemichannels in a cell line derived from human lens epithelial cells (HLE-B3 cells). Under control conditions (recording solution containing Ca^{2+} and Mg^{2+}) the basal rate of Etd uptake was very slow (dotted line), but it increased 1.6 ± 0.1 times in extracellular media nominally-free of Ca^{2+} and Mg^{2+} (DCFS) (Fig. 3A). This result suggests that HLE-B3 cells do have functional hemichannels at their plasma membrane, as it is well known that removal of divalent cations from the extracellular solution increases Cx hemichannel open probability [18,49]. Next, we evaluated the effects of the NO donors SNAP, SNP and GSNO on the rate of Etd uptake in the presence of Ca^{2+} and Mg^{2+}. SNP (1.44 ± 0.12 times) and GSNO (1.29 ± 0.17 times) increased the rate of Etd uptake, whereas SNAP had no significant effect (1.07 ± 0.18 times) (Fig. 3A). Since SNP elicited the largest increase, we performed a dose-response analysis (0–500 μM) of its effect. The increase at 50 μM SNP (1.38 ± 0.09 times) was not different from that measured at 500 μM SNP (1.44 ± 0.04 times) (Fig. 3B). When HLE-B3 cells were co-exposed to 500 μM SNP and hemichannel inhibitors (200 μM La^{3+}, 10 μM CORM-2 [50] or 200 μM Gap27) the rate of dye uptake was reduced significantly when compared to the effect of SNP alone. In the presence of La^{3+}, CORM-2 or Gap27 the rates of dye uptake were 1.11 ± 0.05, 1.24 ± 0.07 and 1.22 ± 0.07 times compared to control, respectively (Fig. 3C). SNP releases both NO and cyanide [51]. Given that NO is a gas, the SNP solution over time will be depleted of NO, because its fast degradation rate in saline solution (t_{50} = ~60 min) [52], but will still include cyanide and other metabolites. Cyanide is known to inhibit the cellular metabolism [53], a condition that induce Cx43 hemichannel opening [54]. Hence, to ensure that hemichannel opening does not take place when NO is depleted (negative control), a stock solution of SNP (500 mM) was left at 37 °C for 48 h and non-protected from light in order to remove all the NO but leave all the other metabolites in solution including cyanide. Then HLE cells were exposed to a 500 μM SNP solution obtained from the NO-depleted stock solution. There was a large reduction of the rate of dye uptake in the HLE cells exposed to NO-depleted SNP, to a level of uptake below control conditions (0.78 ± 0.16 times). This suggests that cyanide does not induce hemichannel opening in HLE cells and/or that other metabolites released by SNP, can induce a massive hemichannel closing. All these results suggest that a major fraction of the increase in Etd uptake elicited by SNP occurs through Cx hemichannels.

Then, we studied whether SNP induces Cx46 S-nitrosation in HLE-B3 cells. Cells with or without exposure to SNP were lysed and analyzed by IP using an *anti*-Cx46 antibody attached to magnetic beads, with detection by Western blots using *anti*-SNO antibody. An *anti*-SNO immunoreactive band at ~50 kDa was very faint under control conditions but was clearly apparent in the sample from SNP-treated cells (Fig. 3D, upper blots, right panel). Detection of Cx46 in the same samples indicated that the increase in "S-nitrosation" signal was not due to changes in the amount of Cx46 in the IP sample (Fig. 3D, upper blots, input). These observations were confirmed by comparing IP data from beads without and with primary antibody attached on lysates of cells treated with SNP. When magnetic beads without *anti*-C × 46 were used for IP, no bands were observed in the Western blot probed with *anti*-SNO. In contrast, two evident bands of ~28 and 50 kDa were detected when magnetic beads coupled to *anti*-C × 46 antibody were used (Fig. 3D, lower panels, left blot). When the IP was performed using *anti*-SNO antibody coupled to magnetic beads, Western blots probed with

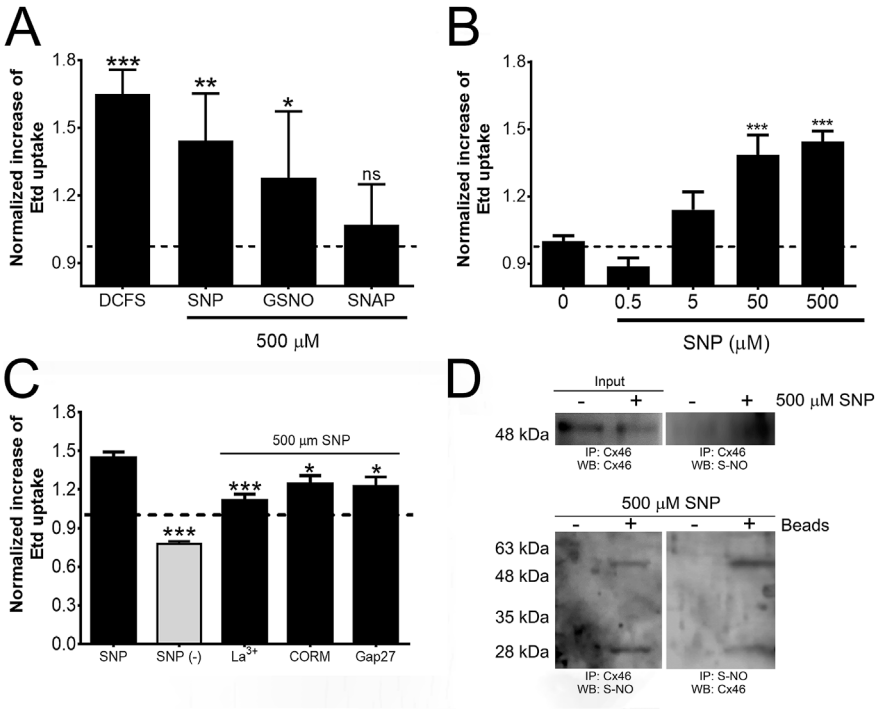

Fig. 3. NO donors increase hemichannel activity and Cx46 S-nitrosation in HLE-B3 cells. (A) Effects of exposure to 500 μM SNP (n = 5), 500 μM GSNO (n = 5) or 500 μM SNAP (n = 3) on Etd uptake in HLE-B3 cells. Cells were grown in glass coverslips to 70–80% confluence and the rate of Etd (10 μM) uptake was measured in time lapse experiments for 20 min. Data were normalized to the rate of Etd uptake under control conditions (dotted line; presence of Ca^{2+} and Mg^{2+} and absence of drugs). For comparison, the maximal rate of Etd uptake through hemichannels was determined in divalent cation-free solution (DCFS). (B) Concentration dependence of the effect of exposure to SNP for 20 min (n = 10 per condition). (C) Inhibition of the effect of SNP by three Cx hemichannel blockers, La^{3+} (200 μM), CORM-2 (10 μM) and Gap27 (200 μM) (n = 3 per inhibitor). As negative control a stock solution of SNP (500 mM) was placed at 37 °C overnight, in the next day was tested the effect of this NO depleted SNP (gray bar, n = 5). (D) S-nitrosation of Cx46. Representative immunoprecipitations (IPs) were analyzed by Western blotting for the presence of Cx46 (WB Cx46) or S-nitrosation (WB S-NO). Top membranes: IP from experiments using beads coupled to *anti*-Cx46 antibody (IP Cx46) probed for the presence of Cx46 (left, IP Cx46/WB Cx46) and S-nitrosation (right, IP Cx46/WB S-NO). Bottom membranes: IP from experiments on lysates from cells treated with SNP using beads without (−) or with conjugated antibody (+). The membrane on the left was probed for the presence of S-nitrosation (IP Cx46/WB S-NO) and that on the right for the presence of Cx46 (IP S-NO/WB Cx46). Data in panels A–C correspond to means ± SEM, *, ** and *** indicate $p < 0.05$, $p < 0.01$ and $p < 0.001$, respectively.

anti-C × 46 antibody also revealed two immunoreactive bands of ~28 and 50 kDa (Fig. 3D, lower panels, right blot). The ~50-kDa band corresponds to full-length Cx46. Considering that the *anti*-Cx46 antibody is directed to the C-terminal region, the ~28-kDa band could be a proteolytic product that contains the C-terminal region and TM4, or result from alternative translation from an internal starting codon. In this context, an alternative use of a starting codon can produce a ~20-kDa version of Cx43 [55]. We were able to identify the equivalent AUG codon in rat and human Cx46, and translation from that site will result in a peptide of ~24 kDa, very similar to the ~28-kDa band in the IP experiments of Fig. 3D. These results show that exposure to NO in human lens cells produces S-nitrosation of Cx46 and increases hemichannel activity.

3.3. Cx46 C-terminus is not necessary for the effect of NO

We have shown that Cx46 hemichannels properties are affected by GSNO [36] and that Cx46 is S-nitrosylated both *in vitro* and *in vivo* (see above). However, the domains and residues that are S-nitrosated and account for the NO donor effects have not been identified. To address that gap in knowledge we determined whether NO donors change the electrophysiological properties of recombinant Cx46 hemichannels expressed in frog oocytes by means of two-electrode voltage clamp recordings. Under normal conditions, Cx46 hemichannels show a small tail current and no current inactivation at high positive voltages (Fig. 4A). After 30-min exposure to 1 mM GSNO, Cx46 hemichannels currents displayed increased tail current and current inactivation at voltages ranging from +50 to +60 mV (Fig. 4B). These results are very similar to those observed previously by our group [36], and to those elicited by 30-min exposure to 1 mM SNAP (Fig. 4C) or 1 mM SNP (Fig. 4D). Since NO affects hCx46 in human lens cells and rCx46 in *Xenopus laevis* oocytes, it seems that the effect of NO on Cx46 hemichannels is independent on the model used, and likely the result of a direct effect on Cx46.

In our previous work we observed that the replacement of cysteine residues 218, 283 and 321 with Ala (Cx46C3A) prevented the effects of

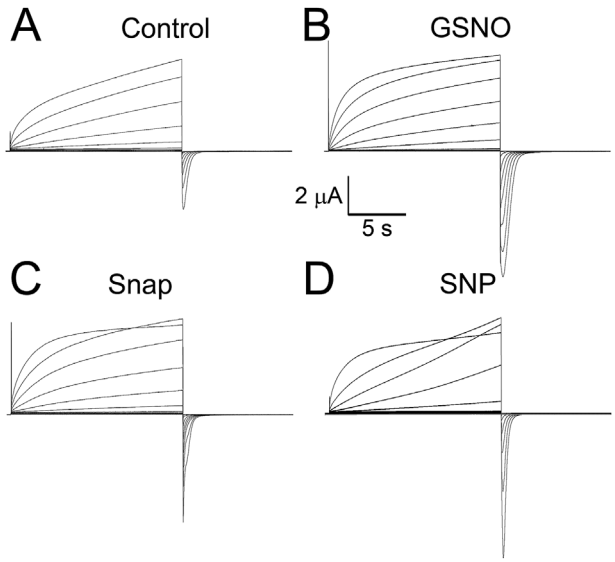

Fig. 4. Nitric oxide donors change the electrophysiological properties of Cx46 hemichannels. Typical examples of whole cell current records from *Xenopus laevis* oocytes expressing Cx46. Hemichannel currents were obtained under control conditions (ND96 solution in the absence of drugs) (A), and after 30 min exposure to 1 mM SNAP (B), SIN-1 (C) or SNP (D). Oocytes were clamped to −60 mV, and for 15 s from −60 mV to +60 mV, in 10-mV steps. At the end of each pulse, the membrane potential was returned to −60 mV for 10 s.

GSNO on Cx46 hemichannels [36]. These data strongly suggest that one or more of these cysteines is/are responsible for sensing the changes in redox potential produced by NO. It is interesting to note that under control conditions hemichannel currents formed by Cx46 truncated in its C-terminus (Cx46ΔCT; C218 present, C283 and C321 absent) resemble those of Cx46 hemichannels after exposure to NO (Fig. 5A, upper left recording), and are not affected by GSNO [36]. One possibility to explain the “S-nitrosated-like” currents and absence of

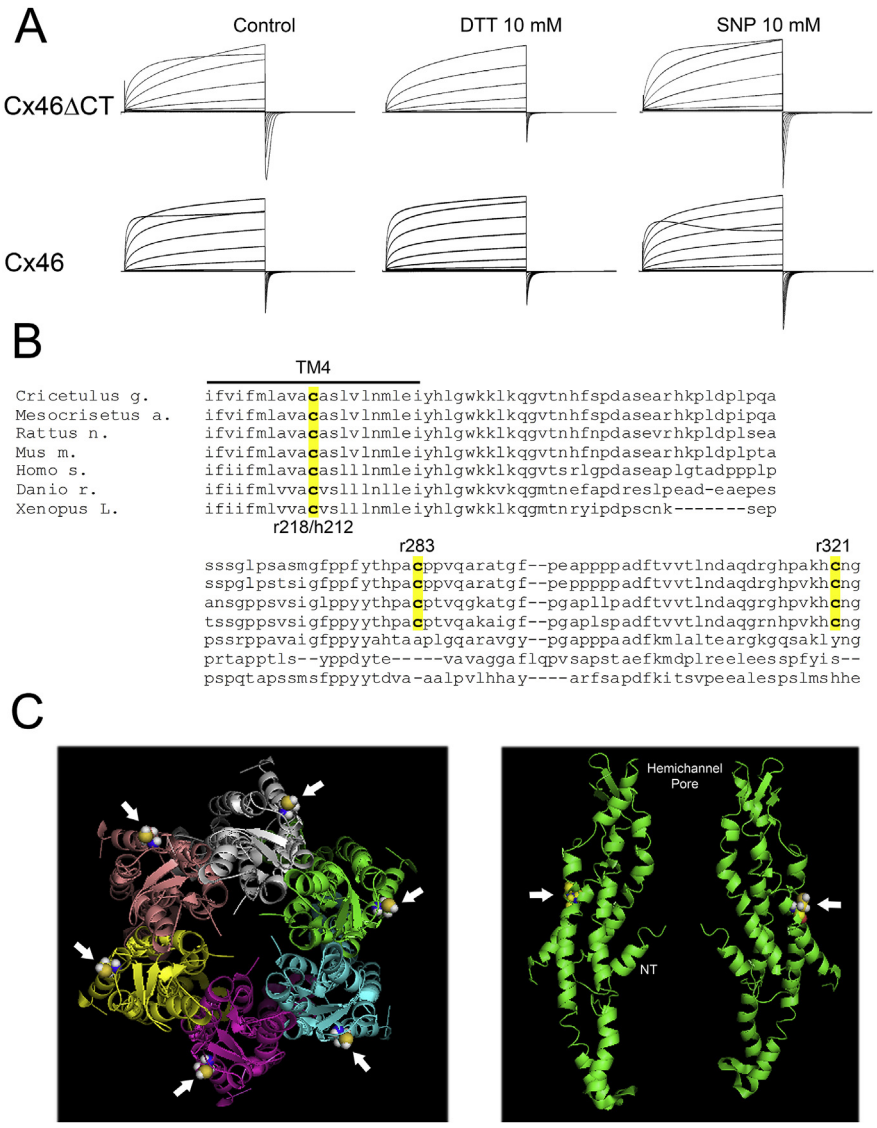

Fig. 5. Cx46ΔCT is sensitive to changes of redox potential. (A) Representative whole cell hemichannel current records from oocytes expressing Cx46ΔCT or Cx46 under control conditions (ND96 in the absence of drugs), after exposure to 10 mM DTT for 30 min, and after subsequent exposure to 1 mM SNP for 30 min. (B) Comparison of Cx46 C-Terminal sequences from different species. Note that only the cysteine equivalent to rat C218 is present in all of them. (C) Molecular simulation of Cx46 suggests that C218 (arrows) faces the membrane lipids.

response to GSNO is that the NO target cysteine in Cx46ΔCT is (are) already oxidized. To test this hypothesis, we exposed the oocytes expressing Cx46ΔCT to the reducing agent DTT. Exposure to 10 mM DTT for at least 30 min eliminated the current inactivation at high voltages and reduced the tail current amplitude (Fig. 5A, upper middle recording). The current inactivation and larger amplitude of the tail current were recovered when these "reduced" Cx46ΔCT hemichannels were exposed to 10 mM SNP for 30 min (Fig. 5A, upper right recording). Under control conditions about 10% of the oocytes expressing Cx46 present basal "oxidized-like" currents (Fig. 5A, lower left recording; compare to typical currents in Fig. 4A). These "oxidized" Cx46 hemichannels presenting current inactivation and larger tail currents can be transformed to a "reduced" form displaying currents without inactivation and with small tail currents by treatment with DTT as described above (Fig. 5A, lower middle). Subsequent exposure to 10 mM SNP for 30 min elicited current inactivation and large tail currents (Fig. 5A, lower right recording). Since the response to reducing and oxidizing agents was observed in Cx46 and Cx46ΔCT hemichannels, it seems that C283 and C321 are not the NO targets, and therefore the results point to C218.

3.4. Transmembrane C218 is a NO target in Cx46 hemichannels

Cysteine at TM4 is highly-conserved in amphibians, fish, rodents and humans (Fig. 5B). Molecular modeling of Cx46 suggests that cysteine faces the membrane lipids (Fig. 5C, white arrow), and therefore, it is possible that the hydrophobic NO solubilized in the membrane lipids is responsible for S-nitrosation of C218. S-nitrosation of cysteine residues in transmembrane domains has been observed in other systems [56]. Predictions of the most likely S-nitrosation of cysteines in Cx46 using the GPS-SNO software (http://sno.biocuckoo.org/down.php) [57] also pointed to C218.

To confirm that C218 is the functionally important target of NO, we studied hemichannels formed by the Cx46-C218A mutant. As previously described [36], and also shown in Fig. 4A, exposure of oocytes expressing Cx46 to 1 mM GSNO yielded currents that displayed current inactivation at +60 mV and a small increase of tail currents (Fig. 6A, left panels). Neither of these changes were observed when C218A hemichannels were exposed to 1 mM GSNO (Fig. 6A, right panels). Moreover, fit of the data to a Boltzmann equation did not show differences in I/V relationship parameters between control and GSNO in

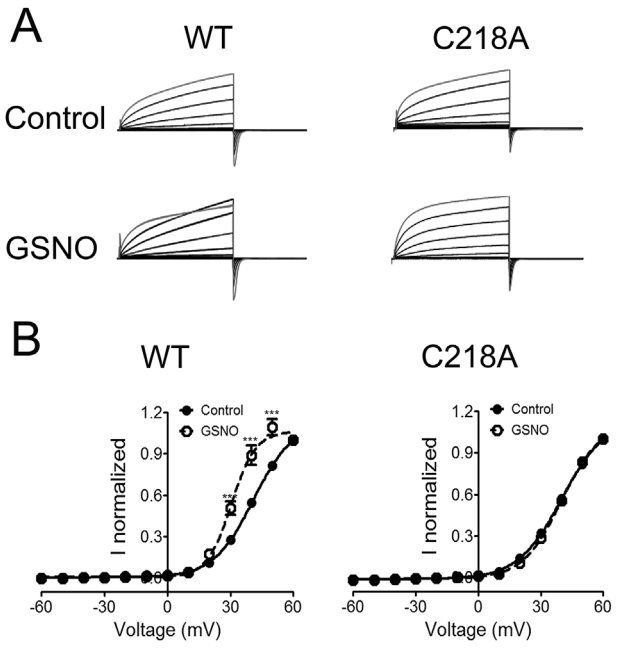

Fig. 6. C218 confers NO sensitivity to rat Cx46 hemichannels. (A) Representative hemichannel currents from *Xenopus* oocytes expressing Cx46 or a mutant lacking C218 (C218A). Records obtained under control conditions (n = 23) or in presence of the NO donor GSNO (1 mM for 20 min, n = 27). (B) I/V relationship for Cx46 and the C218A mutant under control conditions and after exposure to GSNO. Data were normalized to the maximum current measured at +60 mV and then fitted using a Boltzmann equation. Each point represents the mean ± SEM, and *** indicates p < 0.001 vs. control.

C218A hemichannels (Fig. 6B), as it did for the Cx46 HCs I/V relationship (Fig. 6B).

3.5. Cx46 GJC-currents are not affected by a NO donor

We decided to test whether the NO also affects Cx46 GJCs. Unexpectedly, when oocyte pairs where exposed to 10 mM SNP for 10 min we did not observe changes in GJC electrophysiological properties. A simple explanation would be that GJC were already oxidized. However, exposure of the oocyte pairs to 10 mM DTT for 10 min did not affect the Cx46 GJC I/V relationship (Fig. 7). These results suggest that, contrary to Cx46 hemichannels, GJCs formed by Cx46 are not affected by the redox potential.

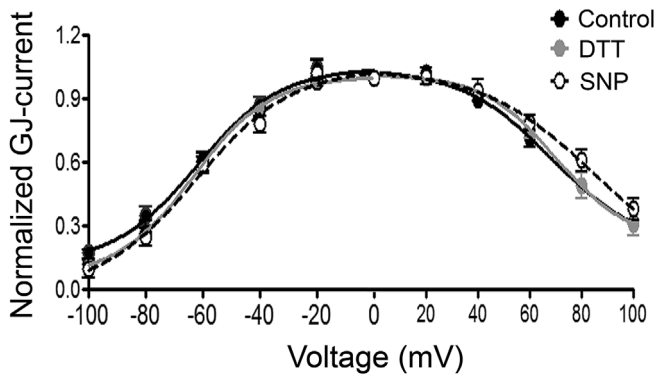

Fig. 7. NO does not affect Cx46 GJCs. Two *Xenopus* oocytes expressing Cx46 were pared overnight and then the cell-to-cell currents were measured under control conditions (filled circles), and after exposure to 10 mM DTT (gray circles) or 10 mM SNAP (open circles) for 10 min (n = 17 for each condition). The data were fitted with a Boltzmann equation.

4. Discussion

In this work we found that lens opacity was correlated *in vivo* with Cx46 S-nitrosation. In agreement with this result, lens HLE-B3 lens cells exposed to NO donors displayed increased hemichannel opening which was also correlated with Cx46 S-nitrosation. Electrophysiological studies performed in *Xenopus laevis* oocytes, revealed that rat Cx46 hemichannels are sensitive to NO donors, and that a cysteine located in TM4 (C218 in rat Cx46; equivalent to human Cx46 C212) is essential for the NO donor effects. The S-nitrosation effect was selective for hemichannels, since NO donors had no effect on Cx46 GJCs.

Cx46 is expressed mainly in the lens where it forms GJCs and hemichannels [58,59]. In lens fiber cells Cx46 hemichannels show a very low open probability at resting potential (−60 mV) [59,60], that is, nevertheless, sufficient to yield a sustained inward current that is completely blocked by 1 mM La^{3+} [60]. Consistent with this, lens fiber cells can uptake molecules such as reduced glutathione, DAPI and propidium through Cx46 hemichannels [59,61]. Although there are no reports on Cx expression and hemichannel function in HLE-B3 cells, it seems that Cx43 and Cx46 are present. This conclusion is based on the partial block of Etd uptake induced by DCFS by Gap27, a blocking peptide selective for Cx43 [62], and that Cx46 was detected in Western blots. Unfortunately, there are no pharmacological tools selective for Cx46 hemichannels that would allow us to confirm Cx46 hemichannel function in the lens cell line. Overall, the available information suggests that Cx46 hemichannels are an important pathway for the flow of small inorganic ions and metabolites across lens fibers, and therefore, an increase in Cx46 hemichannel activity is expected to produce many alterations, including depolarization of the cell membrane, collapse of ionic gradients, increase in Ca^{2+} uptake, loss of organic metabolites, and eventually cell lysis if the increase in activity persists over time. In support of this notion, Cx46 hemichannels with high activity induce cell apoptosis and cataracts development (reviewed by Ref. [24]). In this work, we showed that in a rat selenite model of cataract formation, Cx46 is likely S-nitrosated, and this posttranslational modification was correlated with an increase in hemichannel activity and Cx46 S-nitrosation in HLE-B3 cells. At this time, we cannot distinguish whether Cx46 S-nitrosation causes cataract formation or is a secondary effect. However, it seems possible that a more oxidative redox potential (e.g. diabetes, UV exposure, inflammations) with elevation in NO increases Cx46 S-nitrosation and hemichannel activity, damaging the lens fibers, and resulting in lens opacity.

We found that chemically different NO donors induce similar changes in the properties of rat Cx46 hemichannels expressed in *Xenopus laevis* oocytes, suggesting Cx46 S-nitrosation as a common mechanism, We previously reported that rat Cx46 has two cysteines in its C-terminus (C283 and C321) and one in TM4, all of which could function as NO sensors [36]. In this work we showed that rat Cx46 and Cx46ΔCT are sensitive to NO and DTT, suggesting that the cysteines of the C-terminus are not important as NO sensors. In contrast, mutation of the TM4 cysteine to alanine (C218A) prevented the response to NO, clearly pointing to C218 as the relevant sensor of NO. This conclusion is consistent with the observation that human Cx46 was S-nitrosated in response to a NO donor, even though it does not have cysteines in its C-terminal region. The TM4 cysteine is conserved, suggesting that C218 in rat Cx46 (C212 in the human orthologue) is the NO sensor.

As described under Results, ~90% of the oocytes expressing rat Cx46 show the typical “reduced” phenotype of hemichannel currents characterized by the absence of outward current inactivation at high voltages, smaller tail currents and response to the NO donors. The remaining ~10% of the oocytes show an “oxidized or partially-oxidized” phenotype with outward current inactivation, larger tail currents, slight or lack of response to NO donors and consistent response to DTT. Therefore, when Cx46 hemichannels (and possibly hemichannels formed by other Cx isoforms) are studied, care should be exercised in the evaluation of the redox status as a potentially-important

modulatory factor. Interestingly, the phenotype of the Cx46ΔCT hemichannel currents resembles that of oxidized Cx46 hemichannels. One possibility to explain this observation is that removal of the C-terminal domain induces structural changes in TM4 that promote C218 oxidation.

Most inhibitors and physiologic modulators are not selective, but a few display selectivity between GJCs and hemichannels. Among the latter there are some peptide analogs and aminoglycosides [61–64], which seem to affect only or mostly hemichannels. Although we do not know the molecular bases for the difference, our data show that NO does not affect GJCs formed by rat Cx46 in *Xenopus* oocytes.

Considering previous observations and the results presented here, we propose that Cx46 S-nitrosation could be an important factor in cataracts development due to increased hemichannel opening and/or changes in electrophysiological properties induced by the S-nitrosation of a cysteine located at the TM4.

Acknowledgments

We thank Dr. Lisa Ebihara for providing the Cx46 cDNA. This work was supported by NIH grants [grant number R01GM79629 and 3R01GM079629-03S1] (GAA); The American Heart Association Texas Affiliate Inc. [grant number 14GRNT18750014 (GAA)]; FONDECYT [grant number 1160227 (MAR) and 1160986 (JS)]; Anillo [grant number ACT 1104]; Proyecto interno Universidad del Desarrollo [grant number 23.400.012 (MAR)] and Proyecto Núcleo [grant number UNAB DI-4/17N (JS)].

Appendix A. Supplementary data

Supplementary data to this article can be found online at https://doi.org/10.1016/j.niox.2019.02.007.

References

[1] M. Rackauskas, V. Neverauskas, V.A. Skeberdis, Diversity and properties of connexin gap junction channels, Medicina 46 (2010) 1–12 http://www.ncbi.nlm.nih.gov/pubmed/20234156 , Accessed date: 23 July 2018.
[2] J.E. Contreras, J.C. Saez, F.F. Bukauskas, M.V.L. Bennett, Gating and regulation of connexin 43 (Cx43) hemichannels, Proc. Natl. Acad. Sci. Unit. States Am. 100 (2003) 11388–11393, https://doi.org/10.1073/pnas.1434298100.
[3] S. Bruzzone, L. Guida, E. Zocchi, L. Franco, A. De Flora, Connexin 43 hemi channels mediate Ca^{2+} -regulated transmembrane NAD^{+} fluxes in intact cells, FASEB J. 15 (2001) 10–12, https://doi.org/10.1096/fj.00-0566fje.
[4] C.E. Stout, J.L. Costantin, C.C.G. Naus, A.C. Charles, Intercellular calcium signaling in astrocytes via ATP release through connexin hemichannels, J. Biol. Chem. 277 (2002) 10482–10488, https://doi.org/10.1074/jbc.M109902200.
[5] Z.-C. Ye, M.S. Wyeth, S. Baltan-Tekkok, B.R. Ransom, Functional hemichannels in astrocytes: a novel mechanism of glutamate release, J. Neurosci. 23 (2003) 3588–3596 http://www.ncbi.nlm.nih.gov/pubmed/12736329 , Accessed date: 1 August 2018.
[6] P.P. Cherian, A.J. Siller-Jackson, S. Gu, X. Wang, L.F. Bonewald, E. Sprague, J.X. Jiang, Mechanical strain opens connexin 43 hemichannels in osteocytes: a novel mechanism for the release of prostaglandin, Mol. Biol. Cell 16 (2005) 3100–3106, https://doi.org/10.1091/mbc.e04-10-0912.
[7] J.C. Sáez, K.A. Schalper, M.A. Retamal, J.A. Orellana, K.F. Shoji, M.V.L. Bennett, Cell membrane permeabilization via connexin hemichannels in living and dying cells, Exp. Cell Res. 316 (2010), https://doi.org/10.1016/j.yexcr.2010.05.026.
[8] M.A. Retamal, E.P. Reyes, I.E. García, B. Pinto, A.D. Martínez, C. González, Diseases associated with leaky hemichannels, Front. Cell. Neurosci. 9 (2015), https://doi.org/10.3389/fncel.2015.00267.
[9] J.L. Solan, P.D. Lampe, Spatio-temporal regulation of connexin43 phosphorylation and gap junction dynamics, Biochim. Biophys. Acta Biomembr. 1860 (2018) 83–90, https://doi.org/10.1016/j.bbamem.2017.04.008.
[10] P.D. Lampe, A.F. Lau, Regulation of gap junctions by phosphorylation of connexins, Arch. Biochem. Biophys. 384 (2000) 205–215, https://doi.org/10.1006/abbi.2000.2131.
[11] M.A. Retamal, Connexin and Pannexin hemichannels are regulated by redox potential, Front. Physiol. 5 (2014), https://doi.org/10.3389/fphys.2014.00080 FEB.
[12] M.A. Retamal, C.J. Cortés, L. Reuss, M.V.L. Bennett, J.C. Sáez, S-nitrosylation and permeation through connexin 43 hemichannels in astrocytes: induction by oxidant stress and reversal by reducing agents, Proc. Natl. Acad. Sci. U. S. A 103 (2006), https://doi.org/10.1073/pnas.0511118103.
[13] M.A. Retamal, I.E. García, B.I. Pinto, A. Pupo, D. Báez, J. Stehberg, R. Del Rio, C. González, Extracellular cysteine in connexins: role as redox sensors, Front. Physiol. 7 (2016), https://doi.org/10.3389/fphys.2016.00001.
[14] A. Pfahnl, G. Dahl, Localization of a voltage gate in Connexin46 gap junction hemichannels, Biophys. J. 75 (1998) 2323–2331, https://doi.org/10.1016/S0006-3495(98)77676-3.
[15] T.A. Bargiello, S. Oh, Q. Tang, N.K. Bargiello, T.L. Dowd, T. Kwon, Gating of Connexin Channels by transjunctional-voltage: conformations and models of open and closed states, Biochim. Biophys. Acta Biomembr. 1860 (2018) 22–39, https://doi.org/10.1016/j.bbamem.2017.04.028.
[16] J. Kronengold, M. Srinivas, V.K. Verselis, The N-terminal half of the connexin protein contains the core elements of the pore and voltage gates, J. Membr. Biol. 245 (2012) 453–463, https://doi.org/10.1007/s00232-012-9457-z.
[17] J.M. Gomez-Hernandez, M. de Miguel, B. Larrosa, D. Gonzalez, L.C. Barrio, Molecular basis of calcium regulation in connexin-32 hemichannels, Proc. Natl. Acad. Sci. Unit. States Am. 100 (2003) 16030–16035, https://doi.org/10.1073/pnas.2530348100.
[18] L. Ebihara, X. Liu, J.D. Pal, Effect of external magnesium and calcium on human Connexin46 hemichannels, Biophys. J. 84 (2003) 277–286, https://doi.org/10.1016/S0006-3495(03)74848-6.
[19] B.I. Pinto, A. Pupo, I.E. García, K. Mena-Ulecia, A.D. Martínez, R. Latorre, C. Gonzalez, Calcium binding and voltage gating in Cx46 hemichannels, Sci. Rep. 7 (2017) 15851, https://doi.org/10.1038/s41598-017-15975-5.
[20] M.A. Retamal, F. Evangelista-Martínez, C.G. León-Paravic, G.A. Altenberg, L. Reuss, Biphasic effect of linoleic acid on connexin 46 hemichannels, Pflugers Arch. Eur. J. Physiol. 461 (2011), https://doi.org/10.1007/s00424-011-0936-3.
[21] C. Puebla, M.A. Retamal, R. Acuña, J.C. Sáez, Regulation of Connexin-based channels by fatty acids, Front. Physiol. 8 (2017), https://doi.org/10.3389/fphys.2017.00011.
[22] C. D'hondt, J. Iyyathurai, M. Vinken, V. Rogiers, L. Leybaert, B. Himpens, G. Bultynck, Regulation of connexin- and pannexin-based channels by post-translational modifications, Biol. Cell. 105 (2013) 373–398, https://doi.org/10.1111/boc.201200096.
[23] L.N. Axelsen, K. Calloe, N.-H. Holstein-Rathlou, M.S. Nielsen, Managing the complexity of communication: regulation of gap junctions by post-translational modification, Front. Pharmacol. 4 (2013) 130, https://doi.org/10.3389/fphar.2013.00130.
[24] E.C. Beyer, V.M. Berthoud, Connexin hemichannels in the lens, Front. Physiol. 5 (2014) 20, https://doi.org/10.3389/fphys.2014.00020.
[25] L. Chen, D. Su, S. Li, L. Guan, C. Shi, D. Li, S. Hu, X. Ma, The connexin 46 mutant (V44M) impairs gap junction function causing congenital cataract, J. Genet. 96 (2017) 969–976 http://www.ncbi.nlm.nih.gov/pubmed/29321356 , Accessed date: 1 August 2018.
[26] V.M. Berthoud, P.J. Minogue, H. Yu, J.I. Snabb, E.C. Beyer, Connexin46fs380 causes progressive cataracts, Investig. Opthalmology Vis. Sci. 55 (2014) 6639, https://doi.org/10.1167/iovs.14-15012.
[27] Q. Ren, M.A. Riquelme, J. Xu, X. Yan, B.J. Nicholson, S. Gu, J.X. Jiang, Cataract-Causing mutation of human connexin 46 impairs gap junction, but increases hemichannel function and cell death, PLoS One 8 (2013) e74732, , https://doi.org/10.1371/journal.pone.0074732.
[28] V.M. Berthoud, E.C. Beyer, Oxidative stress, lens gap junctions, and cataracts, Antioxidants Redox Signal. 11 (2009) 339–353, https://doi.org/10.1089/ars.2008.2119.
[29] N. Nagai, Y. Ito, N. Takeuchi, Effect of disulfiram eye drops on lipid peroxide formation via excessive nitric oxide in lenses of hereditary cataract ICR/f rats, Biol. Pharm. Bull. 31 (2008) 981–985 http://www.ncbi.nlm.nih.gov/pubmed/18451530 , Accessed date: 1 August 2018.
[30] N. Nagai, Y. Ito, T. Shibata, E. Kubo, H. Sasaki, A positive feedback loop between nitric oxide and amyloid β (1-42) accelerates mitochondrial damage in human lens epithelial cells, Toxicology 381 (2017) 19–30, https://doi.org/10.1016/j.tox.2017.02.014.
[31] C.-L. Kao, C.-K. Chou, D.-C. Tsai, W.-M. Hsu, J.-H. Liu, C.-S. Wang, J.-C. Lin, C.-C. Wu, C.-H. Peng, C.-J. Chang, C.-L. Kao, S.-H. Chiou, Nitric oxide levels in the aqueous humor in cataract patients, J. Cataract Refract. Surg. 28 (2002) 507–512 http://www.ncbi.nlm.nih.gov/pubmed/11973099 , Accessed date: 12 August 2018.
[32] S.D. Varma, K.R. Hegde, Susceptibility of the ocular lens to nitric oxide: implications in cataractogenesis, J. Ocul. Pharmacol. Therapeut. 23 (2007) 188–195, https://doi.org/10.1089/jop.2006.0124.
[33] J. Kim, C.-S. Kim, E. Sohn, H. Kim, I.-H. Jeong, J.S. Kim, Lens epithelial cell apoptosis initiates diabetic cataractogenesis in the Zucker diabetic fatty rat, Graefe's Arch. Clin. Exp. Ophthalmol. 248 (2010) 811–818, https://doi.org/10.1007/s00417-010-1313-1.
[34] A. Yadav, R. Choudhary, S.H. Bodakhe, Role of nitric oxide in the development of cataract formation in CdCl2-induced hypertensive animals, Curr. Eye Res. (2018) 1–11, https://doi.org/10.1080/02713683.2018.1501490.
[35] D.L. Paul, L. Ebihara, L.J. Takemoto, K.I. Swenson, D.A. Goodenough, Connexin46, a novel lens gap junction protein, induces voltage-gated currents in nonjunctional plasma membrane of Xenopus oocytes, J. Cell Biol. 115 (1991) 1077–1089 http://www.ncbi.nlm.nih.gov/pubmed/1659572 , Accessed date: 20 April 2018.
[36] M.A. Retamal, S. Yin, G.A. Altenberg, L. Reuss, Modulation of Cx46 hemichannels by nitric oxide, Am. J. Physiol. Cell Physiol. 296 (2009), https://doi.org/10.1152/ajpcell.00054.2009.
[37] N. Li, Y. Zhu, X. Deng, Y. Gao, Y. Zhu, M. He, Protective effects and mechanism of tetramethylpyrazine against lens opacification induced by sodium selenite in rats, Exp. Eye Res. 93 (2011) 98–102, https://doi.org/10.1016/j.exer.2011.05.001.
[38] B. Button, L. Reuss, G.A. Altenberg, PKC-mediated stimulation of amphibian CFTR depends on a single phosphorylation consensus site. insertion of this site confers

PKC sensitivity to human CFTR, J. Gen. Physiol. 117 (2001) 457–468 http://www.ncbi.nlm.nih.gov/pubmed/11331356 , Accessed date: 1 August 2018.
[39] R. Abagyan, M. Totrov, D. Kuznetsov, ICM?A new method for protein modeling and design: applications to docking and structure prediction from the distorted native conformation, J. Comput. Chem. 15 (1994) 488–506, https://doi.org/10.1002/jcc.540150503.
[40] S. Maeda, S. Nakagawa, M. Suga, E. Yamashita, A. Oshima, Y. Fujiyoshi, T. Tsukihara, Structure of the connexin 26 gap junction channel at 3.5 Å resolution, Nature 458 (2009) 597–602, https://doi.org/10.1038/nature07869.
[41] G.N. Ramachandran, C. Ramakrishnan, V. Sasisekharan, Stereochemistry of polypeptide chain configurations, J. Mol. Biol. 7 (1963) 95–99 http://www.ncbi.nlm.nih.gov/pubmed/13990617 , Accessed date: 1 August 2018.
[42] O. Carugo, Statistical validation of the root-mean-square-distance, a measure of protein structural proximity, Protein Eng. Des. Sel. 20 (2007) 33–37, https://doi.org/10.1093/protein/gzl051.
[43] O.S. Smart, J.G. Neduvelil, X. Wang, B.A. Wallace, M.S. Sansom, HOLE: a program for the analysis of the pore dimensions of ion channel structural models, J. Mol. Graph. 14 (1996) 354–360 376 http://www.ncbi.nlm.nih.gov/pubmed/9195488 , Accessed date: 1 August 2018.
[44] W.L. Jorgensen, J. Chandrasekhar, J.D. Madura, R.W. Impey, M.L. Klein, Comparison of simple potential functions for simulating liquid water, J. Chem. Phys. 79 (1983) 926–935, https://doi.org/10.1063/1.445869.
[45] J.C. Phillips, R. Braun, W. Wang, J. Gumbart, E. Tajkhorshid, E. Villa, C. Chipot, R.D. Skeel, L. Kalé, K. Schulten, Scalable molecular dynamics with NAMD, J. Comput. Chem. 26 (2005) 1781–1802, https://doi.org/10.1002/jcc.20289.
[46] V.M. Berthoud, A. Ngezahayo, Focus on lens connexins, BMC Cell Biol. 18 (2017) 6, https://doi.org/10.1186/s12860-016-0116-6.
[47] N.J. Russell, J.E. Royland, E.L. McCawley, T.R. Shearer, Ultrastructural study of selenite-induced nuclear cataracts, Invest. Ophthalmol. Vis. Sci. 25 (1984) 751–757 http://www.ncbi.nlm.nih.gov/pubmed/6724845 , Accessed date: 1 August 2018.
[48] P.J. Avarachan, U.M. Rawal, Protein profile in the progressive experimental cataract (selenite model)., Indian J. Ophthalmol. 33 (n.d.) 303–8.http://www.ncbi.nlm.nih.gov/pubmed/3843340(accessed August 1, 2018).
[49] V.K. Verselis, M. Srinivas, Divalent cations regulate connexin hemichannels by modulating intrinsic voltage-dependent gating, J. Gen. Physiol. 132 (2008) 315–327, https://doi.org/10.1085/jgp.200810029.
[50] C.G. León-Paravic, V.A. Figueroa, D.J. Guzmán, C.F. Valderrama, A.A. Vallejos, M.C. Fiori, G.A. Altenberg, L. Reuss, M.A. Retamal, Carbon monoxide (CO) is a novel inhibitor of connexin hemichannels, J. Biol. Chem. 289 (2014), https://doi.org/10.1074/jbc.M114.602243.
[51] M. Yamada, K. Momose, E. Richelson, M. Yamada, Sodium nitroprusside-induced apoptotic cellular death via production of hydrogen peroxide in murine neuroblastoma N1E-115 cells, J. Pharmacol. Toxicol. Methods 35 (1996) 11–17 http://www.ncbi.nlm.nih.gov/pubmed/8645875 , Accessed date: 1 February 2019.
[52] O.R. Leeuwenkamp, E.J. van der Mark, W.P. van Bennekom, A. Bult, Investigation of the photochemical and thermal degradation of aqueous nitroprusside solutions using liquid chromatography, Int. J. Pharm. 24 (1985) 27–41, https://doi.org/10.1016/0378-5173(85)90142-5.
[53] D.H. Jang, F.S. Shofer, S.L. Weiss, L.B. Becker, Impairment of mitochondrial respiration following *ex vivo* cyanide exposure in peripheral blood mononuclear cells, Clin. Toxicol. 54 (2016) 303–307, https://doi.org/10.3109/15563650.2016.1139712.
[54] S.A. John, R. Kondo, S.Y. Wang, J.I. Goldhaber, J.N. Weiss, Connexin-43 hemichannels opened by metabolic inhibition, J. Biol. Chem. 274 (1999) 236–240 http://www.ncbi.nlm.nih.gov/pubmed/9867835 , Accessed date: 1 February 2019.
[55] E. Leithe, M. Mesnil, T. Aasen, The connexin 43 C-terminus: a tail of many tales, Biochim. Biophys. Acta Biomembr. 1860 (2018) 48–64, https://doi.org/10.1016/j.bbamem.2017.05.008.
[56] P.C. Leclerc, P.M. Lanctot, M. Auger-Messier, E. Escher, R. Leduc, G. Guillemette, S-nitrosylation of cysteine 289 of the AT1 receptor decreases its binding affinity for angiotensin II, Br. J. Pharmacol. 148 (2006) 306–313, https://doi.org/10.1038/sj.bjp.0706725.
[57] Y. Xue, Z. Liu, X. Gao, C. Jin, L. Wen, X. Yao, J. Ren, GPS-SNO: computational prediction of protein S-nitrosylation sites with a modified GPS algorithm, PLoS One 5 (2010) e11290, , https://doi.org/10.1371/journal.pone.0011290.
[58] V.M. Berthoud, A. Ngezahayo, Focus on lens connexins, BMC Cell Biol. 18 (2017) 6, https://doi.org/10.1186/s12860-016-0116-6.
[59] L. Ebihara, J.-J. Tong, B. Vertel, T.W. White, T.-L. Chen, Properties of connexin 46 hemichannels in dissociated lens fiber cells, Investig. Opthalmol. Vis. Sci. 52 (2011) 882, https://doi.org/10.1167/iovs.10-6200.
[60] L. Ebihara, Y. Korzyukov, S. Kothari, J.-J. Tong, Cx46 hemichannels contribute to the sodium leak conductance in lens fiber cells, Am. J. Physiol. Cell Physiol. 306 (2014), https://doi.org/10.1152/ajpcell.00353.2013 C506–C513.
[61] W. Shi, M.A. Riquelme, S. Gu, J.X. Jiang, Connexin hemichannels mediate glutathione transport and protect lens fiber cells from oxidative stress, J. Cell Sci. 131 (2018), https://doi.org/10.1242/jcs.212506 jcs212506.
[62] N. Wang, M. De Bock, G. Antoons, A.K. Gadicherla, M. Bol, E. Decrock, W.H. Evans, K.R. Sipido, F.F. Bukauskas, L. Leybaert, Connexin mimetic peptides inhibit Cx43 hemichannel opening triggered by voltage and intracellular Ca2+ elevation, Basic Res. Cardiol. 107 (2012) 304, https://doi.org/10.1007/s00395-012-0304-2.
[63] J. Willebrords, M. Maes, S. Crespo Yanguas, M. Vinken, Inhibitors of connexin and pannexin channels as potential therapeutics, Pharmacol. Ther. 180 (2017) 144–160.
[64] V.K. Verselis, M. Srinivas, Connexin channel modulators and their mechanisms of action, Neuropharmacology 75 (2013) 517–524.